

## A pH-Tunable Nanofluidic Diode: Electrochemical Rectification in a Reconstituted Single Ion Channel

Antonio Alcaraz,<sup>†</sup> Patricio Ramírez,<sup>‡</sup> Elena García-Giménez,<sup>†</sup> M. Lidón López,<sup>†</sup> Andreu Andrio,<sup>†</sup> and Vicente M. Aguilera<sup>\*,†</sup>

Department of Experimental Sciences, Biophysics Unit, University Jaume I, P.O. Box 8029, E-12080 Castellón, Spain, and Department of Applied Physics, Polytechnical University of Valencia, Camino de Vera s/n, E-46022 Valencia, Spain

Received: May 25, 2006; In Final Form: August 22, 2006

We report pH-dependent electrochemical rectification in a protein ion channel (the bacterial porin OmpF) reconstituted on a planar phospholipid membrane. The measurements performed at single-channel level show that the electric current is controlled by the protein fixed charge and it can be tuned by adjusting the local pH. Under highly asymmetric pH conditions, the channel behaves like a liquid diode. Unlike other nanofluidic devices that display also asymmetric conductance, here the microscopic charge distribution of the system can be explored by using the available high-resolution (2.4 Å) channel crystallographic structure. Continuum electrostatics calculations confirm the hypothesized bipolar structure of the system. The selective titration of the channel residues is identified as the underlying physicochemical mechanism responsible for current rectification.

### Introduction

The molecular systems that show rectification (asymmetric conduction) have attracted the attention of researchers, because they are vital components in the development of molecule-based devices that provide faster electronics, higher density data storage, improved methods for drug delivery, and single-molecule analysis.<sup>1,2</sup> The ability of a specific system to produce an asymmetric current–voltage curve depends mainly on the peculiarities of the electrostatic potential spatial profile.<sup>3</sup> Examples include, among others, molecular junctions containing bipolar molecules, chemically modified electrodes, redox-active monolayers,<sup>4,5</sup> or synthetic track-etched nanopores.<sup>1,6</sup> Transmembrane proteins that form ion channels can also play this role as they are highly specialized tools designed to communicate chemically and electrically the living cells with the extracellular environment. There are a number of ion channels that display asymmetric conductance, although its origin may vary greatly. Current rectification of electrostatic nature can be caused by the blocking of the pore by other ions, often divalent cations, asymmetry in permeant ion concentration, and fixed electrical charges or dipoles at the membrane surface or in the channel.<sup>3,7</sup> A remarkable example is the family of inward-rectifying potassium channels in cardiac and neuronal cells.<sup>8</sup>

Here, we report what could be the onset in the development of a molecular diode based on asymmetry in electrostatic interactions. Specifically, we show here that pH-dependent rectification can be achieved by using a lipid membrane reconstituted protein channel, the bacterial porin OmpF (outer membrane protein F) found in the external membrane of *Escherichia Coli*. The OmpF channel has a trimeric structure formed by three

identical and functionally independent subunits. Each monomer opens a wide aqueous pore (see Figure 1), characterized by its poor selectivity and almost no ion specificity. The crystallographic structure of the channel<sup>9</sup> reveals an asymmetric pore geometry, with relatively large entrances and a narrow constriction similar to that of general diffusion porins. Despite the nonsymmetric structure, and the fact that fixed charge is also unevenly distributed along the pore, the channel shows no noticeable rectification unlike other asymmetric channels such as  $\alpha$ -hemolysin.<sup>10–12</sup> Nevertheless, it is shown here that when the pH of both solutions is manipulated, the channel conductive properties are modified and it may become a highly rectifying device. The remarkable feature of the OmpF channel lies on the particularities of the reversible protonation/deprotonation of the channel titratable residues that enables the selection between symmetric and rectifying currents by just adjusting pH. The artificial reconstitution of protein nanopores in unsupported phospholipid bilayers, as we do here, has provided much of our understanding of ion permeation in biological systems but involves a serious limitation for technological applications due to the instability of these membranes. However, recent studies have succeeded in producing robust synthetic scaffolds for protein channels using solid supported membranes, tethered bilayer lipid membranes, or polymerizable lipids. Thus, the idea of protein ion channels acting as components of nanoscale sensors is not an ideal chimera, but has already been achieved in a variety of biotechnological and analytical applications.<sup>13</sup> Our approach could be considered then as the first step in the experimental realization of a recently reported theoretical analysis of nanofluidic diodes,<sup>2</sup> since it is shown here that the OmpF channel may function as a pH-regulated, biological, nanofluidic bipolar diode. On a higher spatial scale, pH-switchable membrane systems have proved to be important for other technological applications such as filtration systems, membrane-based separations, bio-separations, and sensors.<sup>14,15</sup>

\* Corresponding author. Phone: +34-964-728045. Fax: +34-964-728066. E-mail: aguilera@uji.es.

<sup>†</sup> University Jaume I.

<sup>‡</sup> Polytechnical University of Valencia.

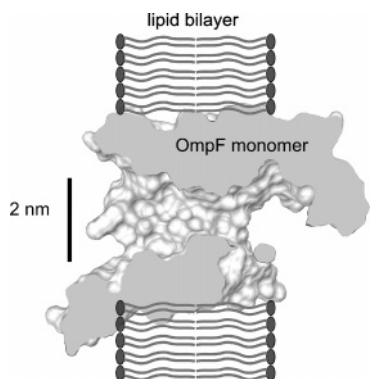


**Figure 1.** Axial section of the OmpF channel superimposed on a cartoon representing the phospholipid planar membrane where the channel is reconstituted. The periplasmic part of the channel is on the left side, and the extracellular part is on the right side.

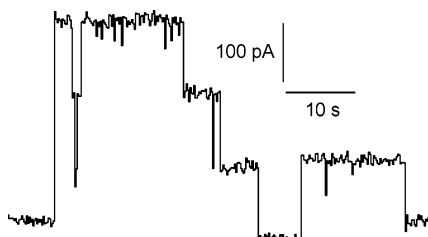


**Figure 2.** Single-channel current recording of OmpF porin reconstituted on a DPhPC planar bilayer. The trimeric nature of the channel is revealed by the spontaneous monomer closures at high applied voltages. Traces shown correspond to measurements performed at pH 7 in 0.1 M KCl and 1 mM  $\text{CaCl}_2$ .

## Methods

**Channel Conductance Measurements.** Wild-type OmpF (a generous gift of Dr. Mathias Winterhalter) was isolated and purified from an *Escherichia coli* culture. Bilayer membranes were formed from two monolayers made from a 1% solution of diphytanoylphosphatidylcholine (DPhPC) (Avanti Polar Lipids, Inc., Alabaster, AL) in pentane (Baker) on 70–80  $\mu\text{m}$  diameter orifices in the 15  $\mu\text{m}$ -thick Teflon partition that separated two chambers.<sup>16,17</sup> The orifices were pretreated with a 1% solution of hexadecane in pentane. The total capacitance depended on the actual location of the orifice in the film (and thus area of the film exposed to salt solution) but was always around 80–120 pF. Aqueous solutions of KCl and 1 mM  $\text{CaCl}_2$  were buffered by 5 mM HEPES. Single-channel insertion was achieved by adding 0.1–0.3  $\mu\text{L}$  of a 1  $\mu\text{g}/\text{mL}$  solution of OmpF in the buffer that contained 1 M KCl and 1% (v/v) of Octyl POE (Alexis, Switzerland) to 2 mL of aqueous phase at the cis side of the membrane only while stirring. The membrane potential was applied using Ag/AgCl electrodes in 2 M KCl, 1.5% agarose bridges assembled within standard 250  $\mu\text{L}$  pipet tips.<sup>16</sup> Potential is defined as positive when it is greater at the side of protein addition (the cis side of the membrane cell). As shown in Figure 2, the formation of OmpF channels is indicated by the characteristic step increases in the current for a given value of the applied potential. An Axopatch 200B amplifier (Axon Instruments, Inc., Foster City, CA) in the voltage-clamp mode was used for measuring the current and applying potential. Data were directly saved into the computer memory. The membrane chamber and the headstage were isolated from external noise sources with a double metal screen (Amuneal Manufacturing Corp., Philadelphia, PA).

**Calculation of Protein Charge Distribution.** The protocol followed to calculate the ionization state of each of the 306

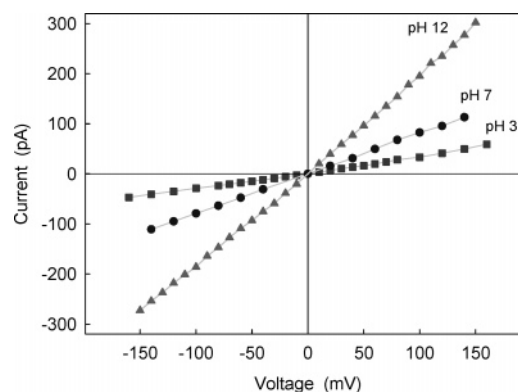


**Figure 3.** Current–voltage curves of OmpF channel in 0.1 M KCl under symmetric pH conditions. No noticeable rectification is observed. There is a 6-fold change in channel conductance from pH 3 to pH 12. Labels indicate the pH on both solutions. Error bars are smaller than the size of the symbols used.

titratable residues in the OmpF channel was described in detail elsewhere.<sup>18,19</sup> To sum, the entire trimer was built using the Protein Data Bank file<sup>9</sup> and was inserted in a membrane represented by a low dielectric medium. The UHBD (the University of Houston Brownian Dynamics Program) code<sup>20,21</sup> was used for the calculation of the  $\text{pK}_a$  of ionizable residues following the procedure described by Antosiewicz et al.<sup>22,23</sup> This approach involves the calculation of the interaction energy between the ionizable groups of the protein and the differences between the ionization energies of each group in the neutral protein and in free solution. All of these energies were assumed to be of purely electrostatic nature so that they could be calculated by means of the Poisson–Boltzmann equation. A Monte Carlo method was later employed for the estimation of the interaction energy between titratable groups.

## Results and Discussion

The ion conduction of OmpF was investigated by reconstituting single channels in planar membranes (made of a neutral lipid, DPhPC). Figure 3 shows the current–voltage ( $I$ – $V$ ) curves of the OmpF channel at basic, neutral, and acidic pH, under symmetrical conditions (the same pH and KCl concentration on both sides of the channel). As seen in the slopes of the measured current–voltage curves, channel conductance is strongly dependent on solution pH, but no rectification is observed. Therefore, it seems that the slight structural asymmetry of the protein channel has a negligible effect on the change of conductance with voltage bias. A tentative explanation for OmpF pH-dependent conductance could be a conformational change inducing an increase in the pore size. However, polymer-partitioning experiments with poly(ethylene glycol) in OmpF channel indicate that the rise in conductance with pH should be attributed to the titration of channel ionizable charges (and the subsequent change in the electric potential distribution) rather than to changes in the effective cross-section of the pore lumen.<sup>24</sup> The fact that the channel geometry is unaffected by pH suggests that the measured  $I$ – $V$  curves are mainly influenced by electrostatic interactions between the permeating ions and the titratable residues within the porin. The pore fixed charges induce local accumulation of charge carriers of opposite sign, so that the ion current is crucially determined by the ionization state of the charged residues in the pore.

To further test the working hypothesis that the channel fixed charge determines its conductance, we manipulated the ionization state of the channel residues in an asymmetric way. The

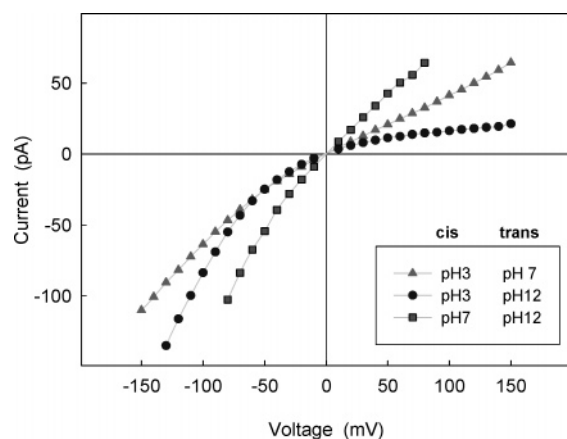


**Figure 4.** Current–voltage curves of OmpF channel in 0.1 M KCl under asymmetric pH conditions show rectification. Labels indicate the pH on the cis side (the side of the protein addition) and the trans side (the side taken as ground for the electric potential).

KCl solutions on either side of the membrane were kept at different pH's. We report here (Figure 4) the results for three different asymmetric pH combinations: (a) acid||neutral (pH 3||pH 7); (b) neutral||basic (pH 7||pH 12); and (c) acid||basic (pH 3||pH 12).

The acid||neutral configuration is obtained with pH 3 in the cis compartment (the side of the protein addition) and pH 7 in the trans compartment. The  $I$ – $V$  curve displays a slope similar to that of the symmetric pH 3||pH 3 configuration (Figure 3) for positive applied voltages, but a clear nonlinearity under negative voltages. The selective titration of some acidic residues in the region of the channel facing the cis side seems responsible for this behavior. This interpretation is supported by detailed electrostatic calculations<sup>18,19</sup> of the  $pK_a$  of ionizable residues present in the channel. Note that when more than 100 ionizable residues per monomer are involved as it is here, the effects of pH on the measured  $I$ – $V$  curves are far from easy to anticipate and these calculations are mandatory. Specifically, the current asymmetry can be ascribed to the neutralization of some negative groups with  $pK_a$  around 4, like aspartic and glutamic acids,<sup>18</sup> which could lead to a positive net charge in the cis side of the channel. The electrostatic nature of this phenomenon is confirmed by a similar rectification found at positive bias for the neutral||acid configuration (not shown here).

The neutral||basic configuration (pH 7 in the cis side and pH 12 in the trans side) shows another asymmetric system obtained by titrating the basic residues in the trans side of the channel. Unlike the acid||neutral configuration, here current rectification seems to be connected to the neutralization of positively charged groups such as lysines, tyrosines, and arginines, yielding an increment in the negative net charge of the channel on the side of high pH. The effect of pH 12 when compared to pH 3 is consistent with the fact that most basic residues facing the pore have  $pK_a$ 's over 12,<sup>18</sup> and thus their titration is only partial.

The most dramatic effect is found for the acid||basic configuration (pH 3 in the cis side and pH 12 in the trans side). Actually, measurements yield a typical diode  $I$ – $V$  curve: a rapid increase of current under negative voltages and a large resistance for positive voltages where current almost attains a limiting value. A similarly shaped  $I$ – $V$  curve is typical of solid-state p–n junctions, polymer ion-exchange bipolar membranes,<sup>25,26</sup> and a number of molecular rectifiers.<sup>2</sup> The selective titration of the channel achieved by partial titration of the acid groups in the cis side, and of the basic residues in the trans side, leads to

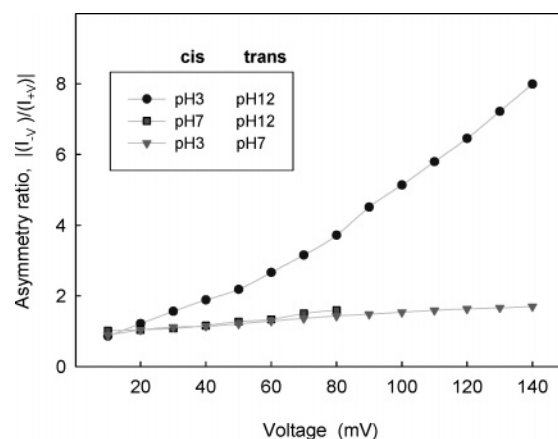


**Figure 5.** Ratio between channel current at negative and positive applied voltages,  $|I(-V)/I(+V)|$ , defined as the rectification ratio in the text. Measurements were performed in 0.1 M KCl under three asymmetric pH conditions (the same as in Figure 4).

a bipolar-type charged system, with a positive net charge in the cis side and a negative net charge in the trans side that are arranged in series. The effect of opposite sign of fixed charge on either side of the channel is best seen in the plot of current rectification ratio at several applied voltages (Figure 5). This ratio is defined as the absolute value of the quotient between currents measured at a given applied potential under both polarities. The pH 3||pH 7 and pH 7||pH 12 configurations yield measurable but moderate rectification, while in the pH 3||pH 12 configuration, the channel current at  $-140$  mV is 8-fold greater than the current at  $140$  mV. Remarkably, the rectification ratio is similar for the two configurations, which share neutral pH on one side. The big difference arises when both sides are titrated in a different way.

At this point, we may wonder whether salt concentration has an effect similar to that of pH on the current rectification ratio. To answer this question and provide further evidence about the role of fixed charges,  $I$ – $V$  measurements were performed under the pH 3||pH 12 configuration using different KCl concentrations. Results are displayed in Figure 6a ( $I$ – $V$  curves) and b (rectification ratio). Interestingly, the rectification ratio decreases as salt concentration increases. This indicates that concentrated solutions screen the channel fixed charges more effectively. Therefore, at high salt concentrations, the different titration on both sides of the channel is less effective and current becomes more similar under both polarities.

As mentioned above, a change in pH modifies not only the channel conductance, but also its selectivity. The OmpF porin is slightly selective to cations at neutral and basic pH, but turns into anion-selective at  $pH < 4$ . This is the key point to understanding how the channel can behave as a bipolar rectifier when it is placed under asymmetric pH conditions. One part of the channel may have an excess of negative net charge, while the other part may have an excess of positive net charge. This appears to be more than a working hypothesis when we focus on the channel atomic structure and perform electrostatic calculations. The ionization state of each channel residue is computed taking into account both the protein dielectric environment and the possible interaction between neighbor residues. Note that the system differs dramatically from most synthetic nanopores where the geometry is usually well defined and often only one type of chemical group is attached to the pore walls. The charge regulation exerted by the pH in a biological channel is then a complicated issue that requires much more detailed calculations than in synthetic systems and make inadequate any

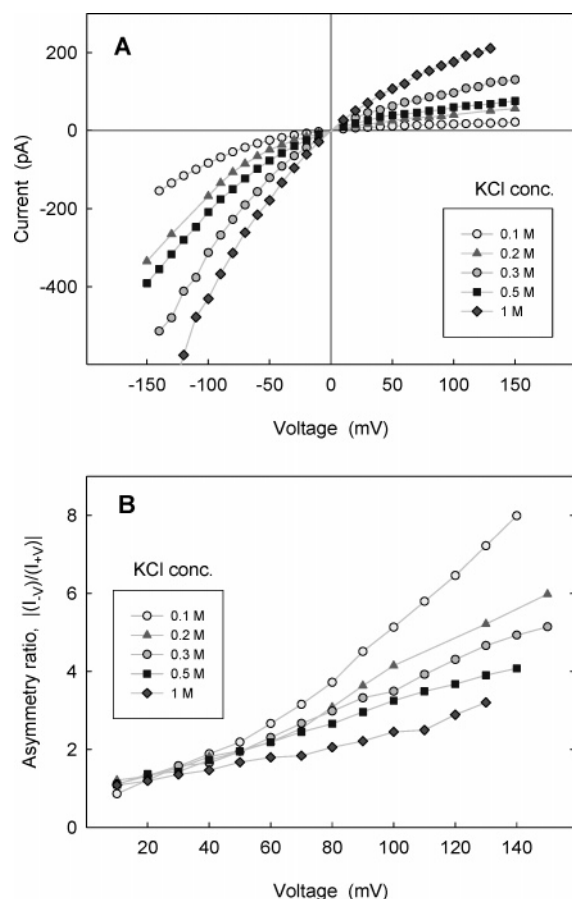


**Figure 6.** (A)  $I$ – $V$  curves of the nanofluidic channel measured under asymmetric pH conditions: pH 3||pH 12 (bipolar configuration). (B) Ratio between channel current at negative and positive applied voltages. Measurements were performed in KCl solutions with concentrations as labeled.

simplistic interpretation. The effective net charge density in the channel, calculated after evaluation of the ionization state of all residues,<sup>18,19</sup> follows the same trend as the measured reversal potential (potential needed to achieve zero current under a salt concentration gradient) when pH is changed (Figure 7a). This correlation indicates that the measured anion selectivity at low pH is consistent with an effective positive charge, whereas the cation selectivity at neutral and basic pH corresponds well with the net negative charge. We can use the information about the charge state of every ionizable residue of the OmpF channel to confirm the bipolar structure of the diode achieved under the acid||basic configuration. Figure 7b shows a ribbon representation of one of the OmpF monomers, based on the atomic structure of the OmpF channel obtained from X-ray crystallography.<sup>9</sup> White and dark gray spheres illustrate the location of the remaining basic and acid residues, respectively, when solution pH is 3 on the left side (periplasmic end) and solution pH is 12 on the right side (extracellular side). The bipolar nature of the system is better visualized by this graphical representation of charged residues. The position of the ionizable residues was taken from the microscopic structure (Protein Data Bank code 2OMF), and their charge state was obtained after the calculation of their corresponding  $pK_a$ .<sup>18</sup> For the sake of clarity, we considered an idealization of the system where pH 3 is considered in the left half of the channel and pH 12 in the right half (in the actual system, the pH changes continuously between both channel ends). As shown, excess positive charge prevails on the channel side facing low pH solution, and there is an excess negative charge on the other side.

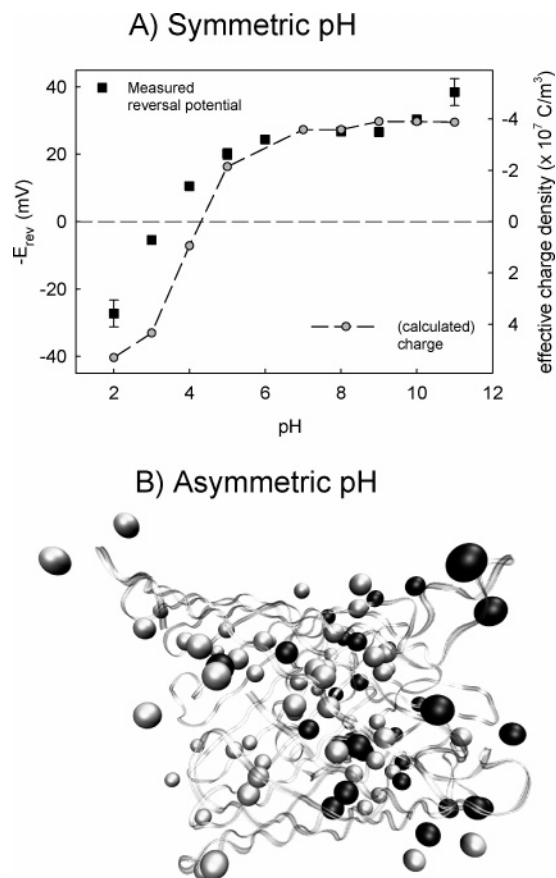


**Figure 7.** (A) OmpF reversal potential (0.1 M KCl trans||1 M KCl cis) and calculated<sup>18</sup> channel effective charge density as a function of pH (the same on both solutions). Positive net charge is consistent with the channel anion selectivity (low pH), and negative net charge is consistent with the cationic selectivity (high pH). (B) Ribbon representation of the OmpF monomer. White and dark gray spheres illustrate the location of the remaining basic and acid residues, respectively, when pH is 3 on the left side (periplasmic end) and pH is 12 on the right side (extracellular side). The position of the ionizable residues was taken from the channel crystallographic structure,<sup>9</sup> and their charge state was obtained after calculation of their respective  $pK_a$ .<sup>18</sup> Excess positive charge prevails on the channel side facing low pH solution, and there is an excess negative charge on the other side.

Figure 8 illustrates the proposed explanation of current rectification in the OmpF channel under the acid||basic configuration. The excess of positive net charge in the side of the channel that faces the acidic solution is equilibrated by a corresponding amount of anions. In the same way, the excess of negative net charge in the other side of the channel, which faces the basic solution, is compensated by a corresponding amount of cations. Under positive applied voltages, the predominant carriers of each zone migrate outward from the channel, heading to the corresponding electrode, giving rise to a depleted zone in the central part of the channel and consequently an increase of electric resistance caused by the lack of ions (see Figure 8a). When the polarity is switched to negative values, we obtain a totally different picture. The excess cations coming from the negative zone try to cross the positive zone and vice versa. The final result is an accumulation of carriers in the central region of the channel (see Figure 8b). The local concentrations become much higher than those in bulk solution, and a rapid increase in current is observed. Note that the asymmetric  $I$ – $V$  curve found in other ion channels such as  $\alpha$ -hemolysin<sup>11,12</sup> does not correspond to the same phenomenon described here, since it appears independently of pH because it is based on the structural asymmetry. Indeed, this  $\alpha$ -hemolysin channel is anion-selective



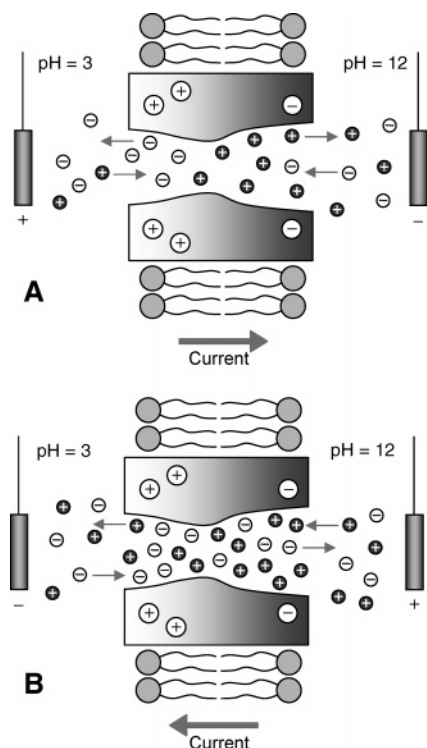


**Figure 8.** Schematic representation of the bipolar diode under positive applied potential (A) and negative bias (B).

for almost the entire pH range (except for  $\text{pH} > 10$ ), and thus its slightly asymmetric  $I$ - $V$  curve (rectification ratio is within the range 1–2) at neutral pH is incompatible with the bipolar picture invoked here.

## Conclusions

We have shown that pH-dependent electrochemical rectification is displayed by a protein ion channel reconstituted in a planar phospholipid membrane. The nonohmic conduction is not associated with channel blocking by ions as happens in other biological channels but seems almost entirely controlled by electrostatic interactions between channel ionizable residues and permeating ions. This allows one to achieve a pH-tunable rectification, and eventually create a bipolar liquid diode. The asymmetric fixed charge distribution arising from the selective titration of the channel residues seems to be the origin of the diode-like ionic conduction. On the one hand, it is emphasized here the crucial role of the electrostatic interactions between the surface charges of the channel and the permeating ions. On the other hand, the experiments reported here open the door to new rectifying devices based on synthetic nanopores, which, after chemical modification, may change their local fixed charge

in response to variation of the pH.<sup>27</sup> Protein channels are being extensively tested as biological sensing elements because of their potential benefits in chemical, pharmaceutical, and biological applications.<sup>13</sup>

**Acknowledgment.** This work was supported by Fundació Caixa-Castelló (project P1-1B2004-27), Generalitat Valenciana (project GV04A/701), and the Spanish Ministry of Education (projects FIS2004-03424 and MAT2006-03097).

## References and Notes

- (1) Schiedt, B.; Healy, K.; Morrison, A. P.; Neumann, R.; Siwy, Z. *Nucl. Instrum. Methods Phys. Res., Sect. B* **2005**, *236*, 109–116.
- (2) Daiguji, H.; Oka, Y.; Shirono, K. *Nano Lett.* **2005**, *5*, 2274–2280.
- (3) Neumcke, B. *Biophysik* **1970**, *6*, 231–240.
- (4) Gasyna, Z. L.; Morales, G. M.; Sanchez, A.; Yu, L. *Chem. Phys. Lett.* **2006**, *417*, 401–405.
- (5) Hwang, S.; Chi, Y. S.; Lee, B. S.; Lee, S. G.; Choi, I. S.; Kwak, J. *Chem. Commun.* **2006**, 183–185.
- (6) Siwy, Z.; Kosińska, I. D.; Fuliński, A.; Martin, C. R. *Phys. Rev. Lett.* **2005**, *94*, 048102.
- (7) Kienker, P. K.; DeGrado, W. F.; Lear, J. D. *Proc. Natl. Acad. Sci. U.S.A.* **1994**, *91*, 4859–4863.
- (8) Oliver, D.; Baukrowitz, T.; Fakler, B. *Eur. J. Biochem.* **2000**, *267*, 5824–5829.
- (9) Cowan, S. W.; Schirmer, T.; Rummel, G.; Steiert, M.; Ghosh, R.; Pauptit, R. A.; Jansonius, J. N.; Rosenbusch, P. J. *Nature* **1992**, *358*, 727–733.
- (10) Kasianowicz, J. J.; Brandin, E.; Branton, D.; Deamer, D. W. *Proc. Natl. Acad. Sci. U.S.A.* **1996**, *93*, 13770–13773.
- (11) Krasilnikov, O. V.; Yuldasheva, L. N.; Merzylak, P. G.; Capistrano, M.-F. P.; Nogueira, R. A. *Biochim. Biophys. Acta* **1997**, *1329*, 51–60.
- (12) Krasilnikov, O. V.; Capistrano, M.-F. P.; Yuldasheva, L. N.; Nogueira, R. A. *J. Membr. Biol.* **1997**, *156*, 157–172.
- (13) Shenoy, D. K.; Barger, W. R.; Singh, A.; Panchal, R. G.; Misakian, M.; Stanford, V. M.; Kasianowicz, J. J. *Nano Lett.* **2005**, *5*, 1181–1185.
- (14) Ramírez, P.; Mafé, S.; Alcaraz, A.; Cervera, J. J. *J. Phys. Chem. B* **2003**, *107*, 13178–13187.
- (15) Park, M. K.; Deng, S.; Advincula, R. C. *J. Am. Chem. Soc.* **2004**, *126*, 13723–13731.
- (16) Bezrukov, S. M.; Vodyanov, I. *Biophys. J.* **1993**, *64*, 16–25.
- (17) Montal, M.; Mueller, P. *Proc. Natl. Acad. Sci. U.S.A.* **1972**, *69*, 3561–3566.
- (18) Alcaraz, A.; Aguilera-Arzo, M.; Nestorovich, E. M.; Aguilera, V. M.; Bezrukov, S. M. *Biophys. J.* **2004**, *87*, 943–957.
- (19) Aguilera-Arzo, M.; García-Celma, J. J.; Cervera, J.; Alcaraz, A.; Aguilera, V. M. *Bioelectrochemistry* **2006**, *71*, 22–29.
- (20) Davis, M. E.; Madura, J. D.; Luty, B. A.; McCammon, J. A. *Comput. Phys. Commun.* **1991**, *62*, 187–197.
- (21) Madura, J. D.; Briggs, J. M.; Wade, R. C.; Davis, M. E.; Luty, B. A.; Ilin, A.; Antosiewicz, J.; Gilson, M. K.; Bagheri, B.; Scott, L. R.; McCammon, J. A. *Comput. Phys. Commun.* **1995**, *91*, 57–95.
- (22) Antosiewicz, J.; McCammon, J. A.; Gilson, M. K. *J. Mol. Biol.* **1994**, *238*, 415–436.
- (23) Antosiewicz, J.; McCammon, J. A. *Biochemistry* **1996**, *35*, 7819–7833.
- (24) Nestorovich, E. M.; Rostovtseva, T. K.; Bezrukov, S. M. *Biophys. J.* **2003**, *85*, 3718–3729.
- (25) Alcaraz, A.; Ramírez, P.; Mafé, S.; Holdik, H.; Bauer, B. *Polymer* **2000**, *41*, 6627–6634.
- (26) Mafé, S.; Ramírez, P. *Acta Polym.* **1997**, *48*, 234–250.
- (27) Fuliński, A.; Kosińska, I. D.; Siwy, Z. *Europhys. Lett.* **2004**, *67*, 683–689.